

# Eastern Bering Sea Ice Dynamics and Thermodynamics

# 13

Carol H. Pease

NOAA  
Pacific Marine Environmental Laboratory  
Seattle, Washington

## ABSTRACT

During winter 1979, hydrographic, meteorological, and ice floe data were collected over the Bering Sea shelf. The ice pack extended to 59° N; however, there appeared to be little or no *in-situ* freezing in the study area. Hydrographic data from the marginal ice region (seaward limit of the ice) showed that less saline, cold ( $\cong -1.4$  C) waters existed in an upper layer; the lower layer was as much as 1 C warmer. Floes advected toward the south to southwest at rates as high as 0.5 m/sec during north-to-northeast wind events. Floes rotted along the margin in periods on the order of days. Little ridging of ice was observed over the open shelf. Rafting was prevalent among floes battered by wind and swell at the ice edge.

We observed that in the fall, northerly winds cool the water of Norton Sound and the Bering Sea north of St. Lawrence Island until the water column is isothermal at freezing temperatures. Further cooling causes freezing. Under northerly wind conditions, ice is advected south into water where it is no longer in thermodynamic equilibrium. The resulting meltwater is mechanically mixed and is a source of cooling for the waters of the southern Bering shelf. These observations suggest that ice formation and movement in the Bering Sea can be likened to a conveyor belt: growth occurs primarily in the north, advection due to wind stress is generally southward, decay occurs at the thermodynamic limit, and the limit advances somewhat as meltwater cools the upper layer.

## INTRODUCTION

On a cruise of the NOAA ship *Surveyor* during the first two weeks of March 1979, many types of oceanographic, meteorologic, and ice floe data were collected in order to identify processes inherent in the distribution and condition of sea ice over the Bering Sea shelf (Fig. 13-1). These data, in conjunction with simultaneous edge-specific studies by Martin and Bauer (Chapter 12, this volume), remote sensing studies by McNutt (Chapter 10, this volume), and previous work by Muench and Ahlnäs (1976) and Ahlnäs and Wendler (1979), yield a well-formed description of mesoscale interaction between dynamics and thermodynamics in controlling the pack ice conditions in the Bering Sea. This chapter describes and presents supporting evidence for this interaction.

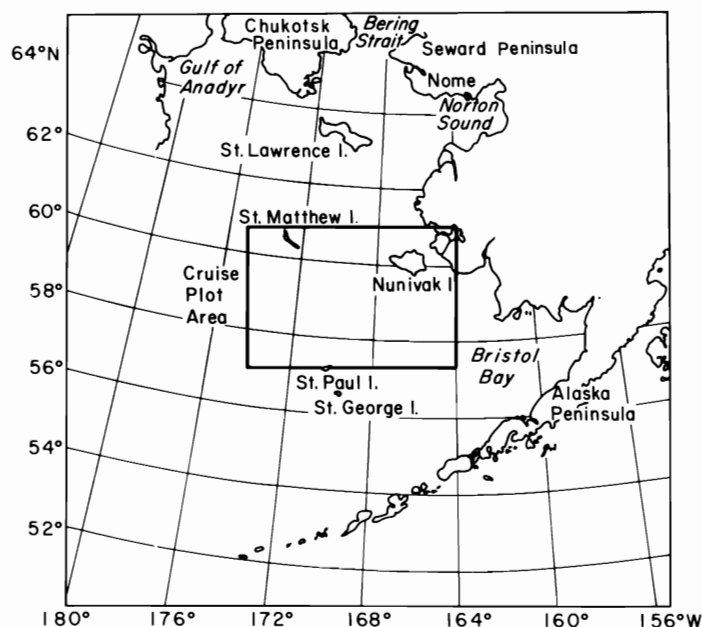


Figure 13-1. Eastern Bering Sea ice study area including the observation area during the cruise of the NOAA ship *Surveyor* during March 1979.

## ICE-EDGE HYDROGRAPHY

Forty-one CTD's (Fig. 13-2) and twenty-two airsondes (Fig. 13-3) were taken along the ice edge during the first two weeks of March 1979 from the NOAA ship *Surveyor*. Oceanic and atmospheric surface temperatures were taken every hour, and surface salinity was taken every two hours. The water temperatures were at first taken as bucket temperatures with a calibrated thermometer ( $\pm 0.2$  C), but after the thermometer was lost, a calibrated

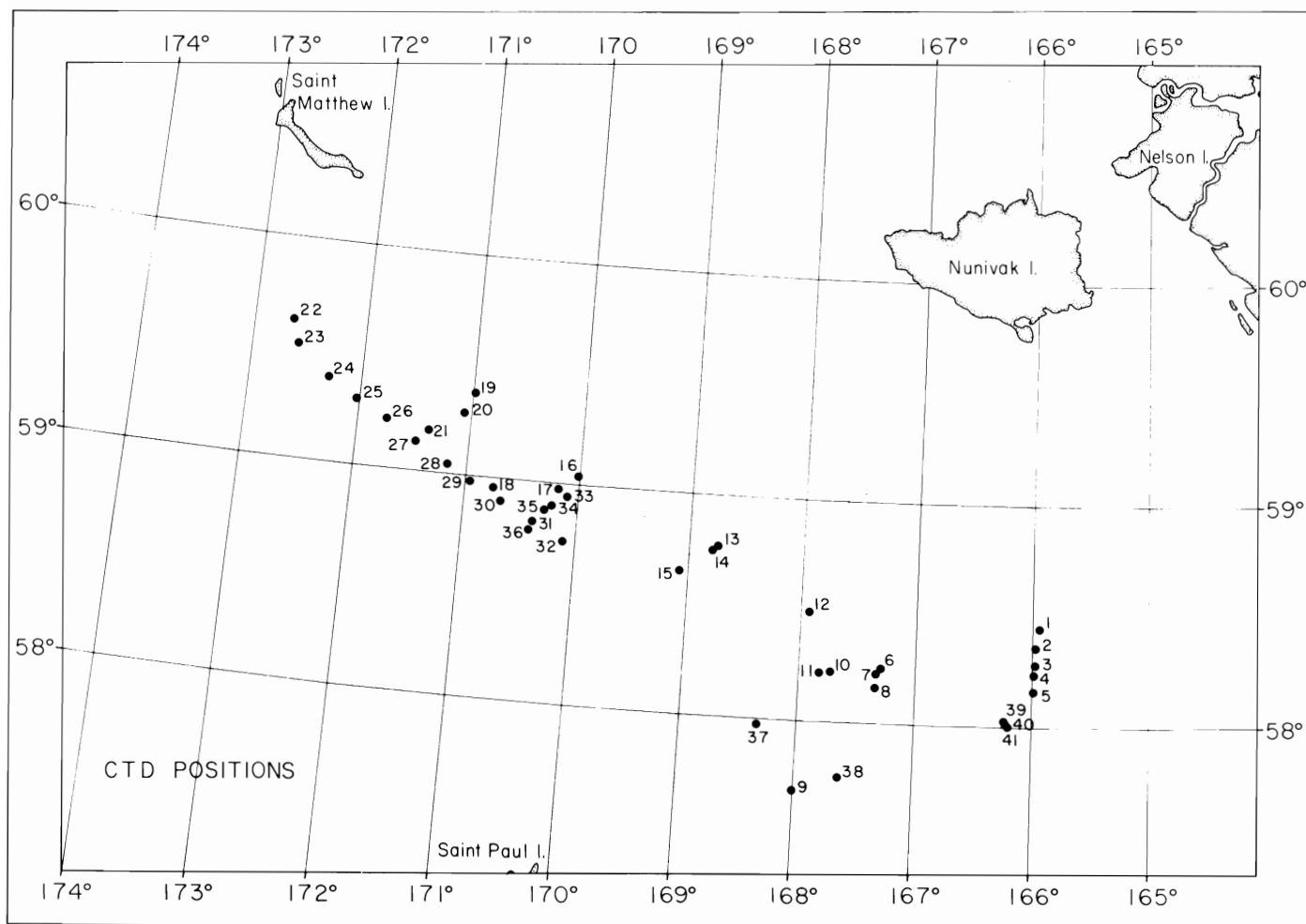


Figure 13-2. The location of CTD stations taken during the first two weeks of March 1979 from the NOAA ship *Surveyor*.

thermistor string ( $\pm 0.1$  C) was used. This method also provided air temperature measurements near the surface. Although temperatures were measured within a few centimeters of the air-sea interface, they are considered representative of more extensive layers since turbulence from the ship's wake provided mechanical mixing. Salinity was determined from bucket samples using an auto-salinometer. With a motorized psychrometer, hourly dry-bulb and air temperatures were taken at the bridge throughout the cruise. However, problems were encountered with the wet-bulb thermometer readings and the data were discarded as unreliable. The bridge measurements were made approximately 10 m above the surface.

In general, the water temperature was above the freezing point of the ice except for that measured in CTD cast No. 1, 80 miles south of Nunivak Island in 30 m of water on March 2. Floes were rotting from the bottom west of this area. Melt puddles were not

formed as in the traditional summer Arctic melt condition, but some floes were wetted when waves washed over them. Details of the mechanical effects of the swell on the ice and resulting edge processes are discussed by Martin and Bauer (Chapter 12, this volume).

A major feature of the water column along the ice edge was fresh cold water due to ice melt. CTD sections perpendicular to the ice edge west of the Nunivak area showed a meltwater lens (Fig. 13-4). The pycnocline downwind of the pack edge was slightly deeper than that under the ice itself, apparently because ice cover protects the water column from wind-mixing; but the exact shape of the front is speculative. The ice in this figure was in surface waters of  $\approx 1.0$  C, although ice was observed in slightly warmer waters at other times.

We also observed the effect of melting by ex-

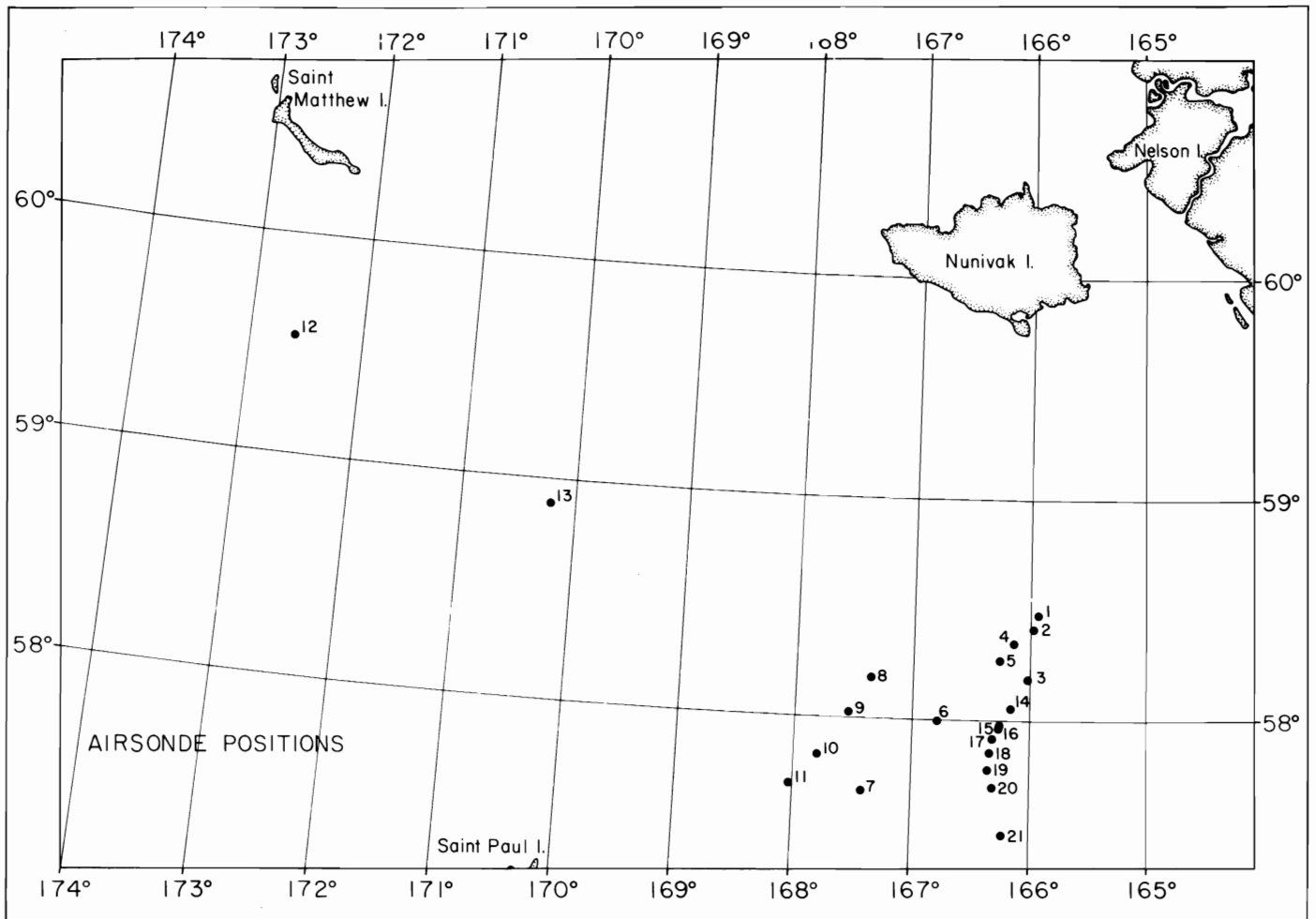


Figure 13-3. The location of radiosonde launches made during the first two weeks of March 1979 from the NOAA ship *Surveyor*.

examining the change in the distribution of sea surface temperature (Fig. 13-5). All surface measurements during the two-week cruise are plotted on the same chart and contoured for the first and second weeks separately. The eastern end of the figure shows the change observed over a two-week period, while the western end shows almost steady-state conditions. Note that while the  $-1.0$  C isotherm moved about 35-40 km south during the cruise, the  $+1.0$  C isotherm did not move appreciably. The salinity field showed the same trend; although the contouring is less significant with only half as many samples (Fig. 13-6), the advance of meltwater is strikingly apparent.

It is possible that movement of meltwater toward the south could be due to advection of the water mass itself. However, the mean currents on the shelf are weak and northwesterly, generally in opposition to the advance of meltwater (Kinder and

Schumacher, Chapter 5, this volume). Contours of dynamic height during the March cruise period also suggest weak flow toward the northwest (Fig. 13-7). Although this dynamic topography has less relief than that shown previously by Charnell et al. (1979), it is similar in inferred speed and direction. Also, the pattern suggested by Figs. 13-5, 13-6, and 13-7 is coherent over periods longer than a tidal cycle.

The amount of ice melt required to lower temperature to observed values (Fig. 13-4) was estimated by assuming that the water had been  $+1.0$  C and that the ice had already warmed to its freezing point. Under these assumptions, enough heat was extracted to melt a 60-km-long, 0.5-m-thick strip of ice of 15‰ salinity. This melt estimate was probably too high since off-ice winds also cool the water, but it shows that the proposed physical mechanism is capable of producing the observed hydrographic features.

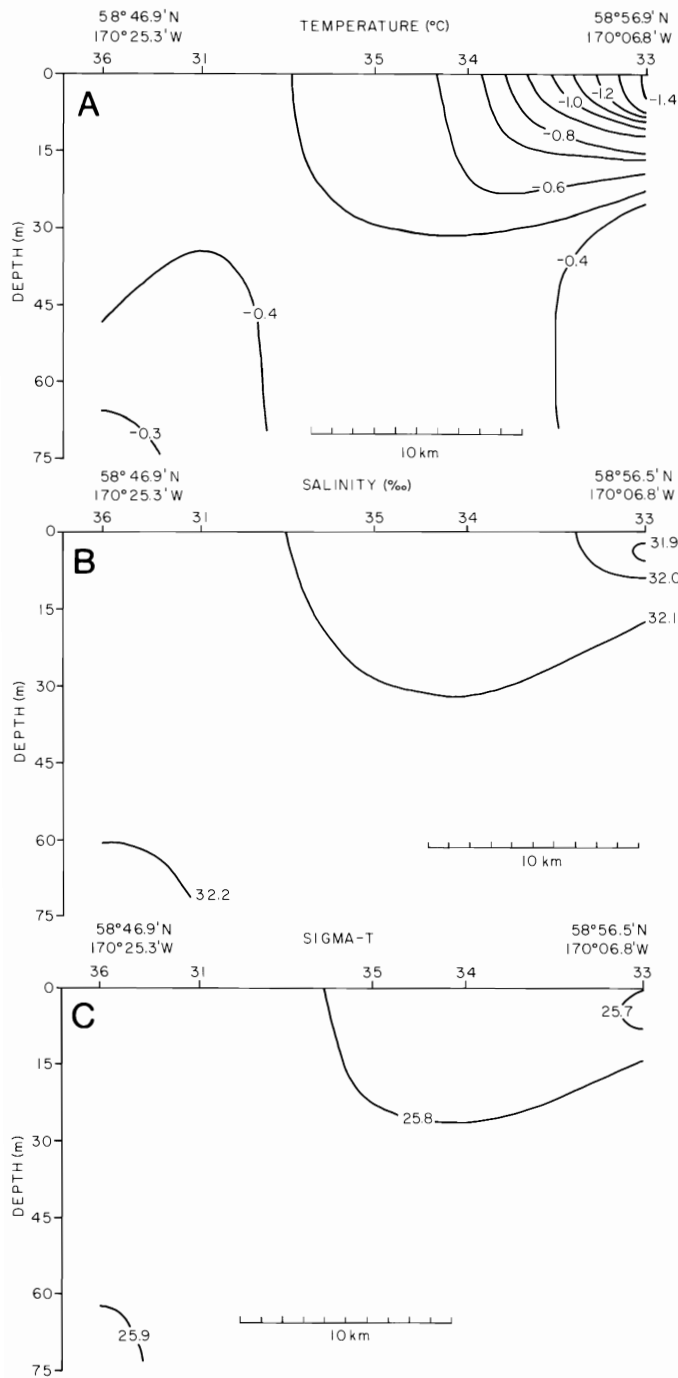


Figure 13-4. A CTD cross section perpendicular to the ice edge showing the meltwater lens typical along the margin of ice. The ice existed in water of about  $-1.0$  C and colder. The CTD station numbers correspond to those in Fig. 13-2.

## DISCUSSION

Ice forms *in situ* during a typical ice-year in late fall (November-December) in Norton Sound, in the

Bering Sea north of St. Lawrence Island, along the Alaskan coast, and eventually southward into Bristol Bay (Fleet Weather Facility 1972-1975, 1976, 1977, and 1978). These areas are shallow (less than 30 m), except for the region north of St. Lawrence Island, and water is observed to be isothermal at the freezing point (about  $-1.7$  C). Cooling is caused by a negative radiation balance and sensible and latent heat transfer due to offshore winter winds. Under the influence of northerly to easterly winds, the ice floes are transported into warmer water. The leading floes melt, adding relatively cold, fresh water to the existing water column. Under continued northerly winds, the new leading floes encounter colder waters and thus have longer residence times. As the season progresses, regions of ice growth expand and the floes are continuously advected beyond these areas.

Satellite and aircraft photographs of the Bering Sea in winter show persistent polynyas in the lee of Cape Nome and St. Lawrence, St. Matthew, and Nunivak Islands during periods of northerly to northeasterly winds (Muench and Ahlnäs 1976, and McNutt, Chapter 10, this volume). Less commonly, a polynya can also be observed in eastern Norton Sound during more easterly wind events. Gray streaks, which Martin and Kauffman (1979) attribute to grease ice production, are often observed in satellite images of these polynyas. Floes 0.3-0.5 m thick near the ice edge but not yet rafted are formed of frazil in approximately the upper half, while the lower half grows in place as columnar crystals (Martin and Kauffman 1979). This indicates that floes continued to grow for a time after the grease ice had consolidated. Overflights show that the floes do not change much in thickness after they are advected away from shore and south of about  $62^{\circ}$ N until they are rafted and melted at the pack edge. Thus, we see areas of growth, relative thermal stability and transport, and thermal and mechanical destruction. These roughly correspond to the regions described by Muench and Ahlnäs (1976) in the spring of 1974. Because of these characteristics, the ice can advance 200-300 km beyond the fall growth region, while the growth region itself expands about 100-200 km beyond its fall extent.

Spring is heralded in the Bering Sea by shifting of the storm tracks north from the Gulf of Alaska to the southern Bering Sea (Overland, Chapter 2, this volume). Given sufficient time, the radiation balance alone would melt the ice pack, but the shifting of the winds from cold northerly to warm southerly can accelerate this procedure considerably. The entire pack can become uniformly rotten in three or four weeks after low-pressure systems penetrate the southern Bering Sea. A wind field during rotting

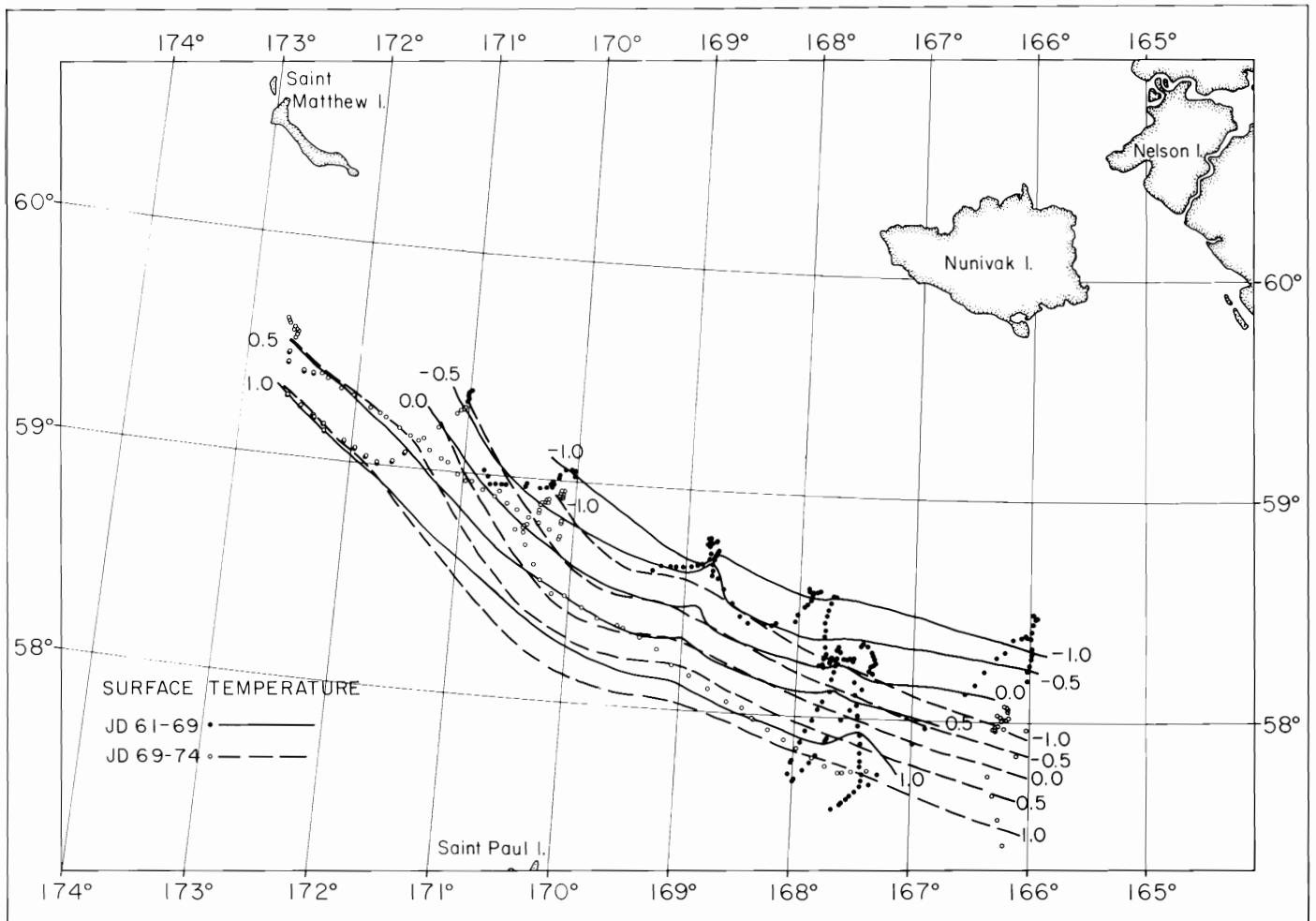


Figure 13-5. Hourly surface water temperatures between 2 March (JD-61) and 15 March (JD-74) 1979 from the NOAA ship *Surveyor*, contoured for the westward and eastward treks respectively. Note that the +1.0 C isotherm did not move significantly while the -1.0 C isotherm moved 35-40 km due to the inclusion of meltwater.

conditions occurred in late March 1979 (Fig. 13-8). The accelerated rotting was observed in winter 1974, a year with extensive ice cover (Muench and Ahlnäs 1976), and in 1979, a year with light ice cover (McNutt, Chapter 10, this volume).

The sea ice is generally divergent on the open Bering shelf because the wind field is slightly divergent when winds are northeasterly and the basin is less constrictive downwind. A northeasterly wind field occurred in early March 1979 (Fig. 13-9). The divergence resulted in little or no ridging of Bering Sea ice compared to the Arctic pack. The few observed ridges formed mainly windward of St. Lawrence Island and in southern Norton Sound. These features generally had low relief because there was little ice to build ridges. Parmenter and Coon (1973) showed that the maximum height of ridges is a function of ice strength and thickness of con-

tributing floes. Since the maximum ridge thickness is about 10 times that of contributing floes, we expect 3-5 m ridges from floes 0.3-0.5 m thick around St. Lawrence Island and possibly 10-20 m ridges from floes 1.0-2.0 m thick in southern Norton Sound.

Vertical water-column structure over the eastern Bering Shelf is complicated. It appears that in areas where the shelf is less than 50 m deep, the entire water column is tidally mixed. In water deeper than 50 m, the structure is two-layered with a pycnocline generally at about 20 m. The upper layer is mixed by wind and the lower layer by tides. Kinder and Schumacher discuss this in detail (Chapter 4, this volume). In ice-growth regions, vertical mixing is enhanced by the extrusion of salt during the freezing process. Since typical ice salinities are 10‰ or greater (Martin and Kauffman 1979), about 20‰ is extruded. A typical advection rate for floes is about

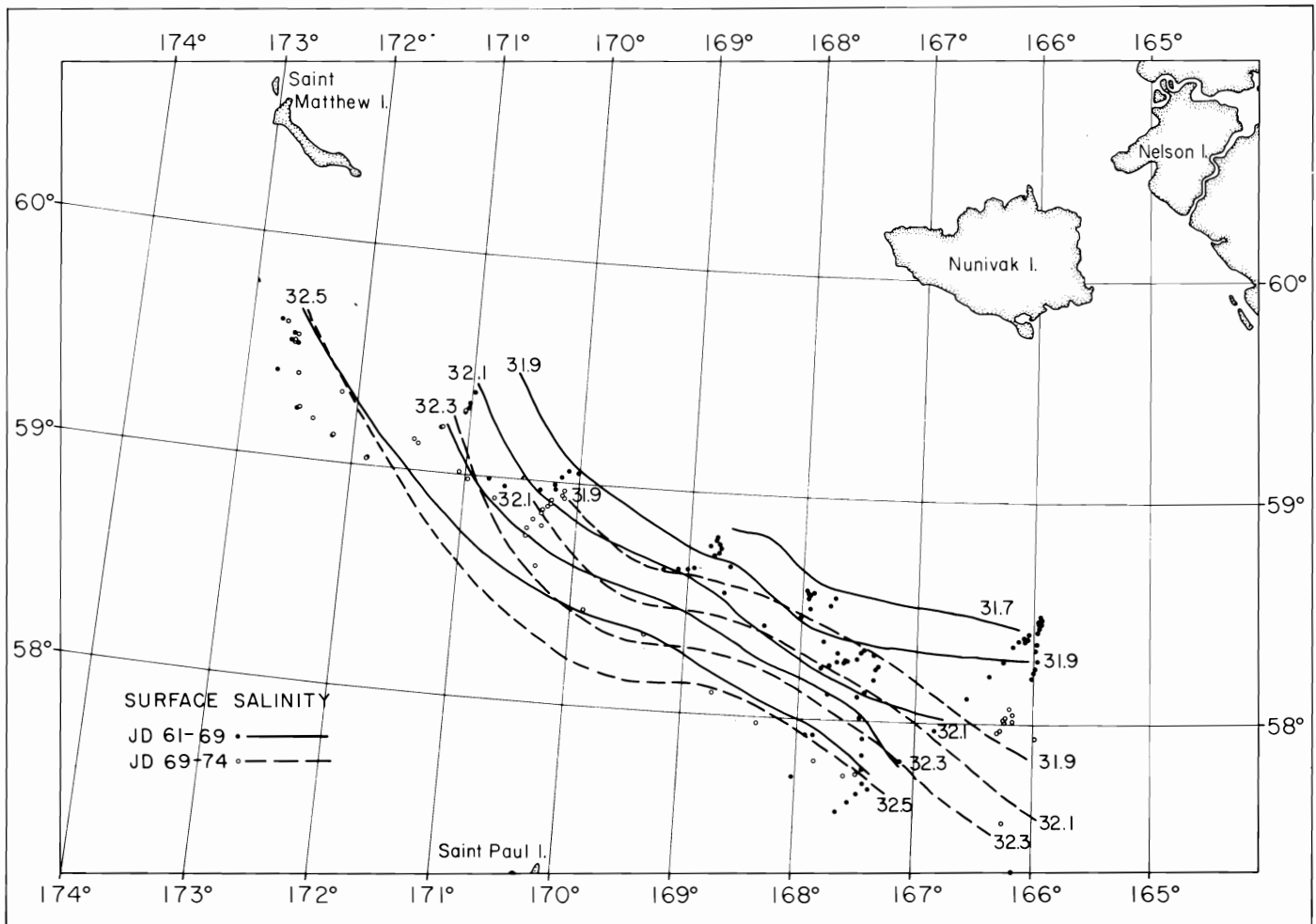


Figure 13-6. Bihourly ocean surface salinities between 2 March (JD-61) and 15 March (JD-74) 1979 from the NOAA ship *Surveyor*, contoured for the westward and eastward treks respectively. Note that the lighter isohalines have moved south during the two-week period while the heavier isohalines have not appreciably moved.

0.25 m/sec (McNutt, Chapter 10, this volume, Muench and Ahlnäs 1976), and we assume steady-state production versus advection of ice 0.3 m thick with a moderately persistent northerly wind regime for about four months. This is equivalent to growing over 5 m of ice in the growth region during the season. Growing this much  $10^0/00$  ice would increase the salinity of 20 m of water by about  $5-6^0/00$  over the season. With different choices for seasonal extent, velocities, and persistence, the range of salinity increase over the season is from  $1.25^0/00$  to  $7.5^0/00$ . However, since the mean current is from the melt zone toward the growth zone, one would expect some of this salt to be recycled, thereby partially masking the salinity-enhancing process. The lower limit of these values is in agreement with those observed by Coachman et al. (1978) for the shoal region southwest of Nunivak Island.

A similar calculation can be made of the number of times the ice pack replaces itself. At a floe speed of 0.25 m/sec, assuming the pack extends 300 km south of Nome and persists for four months, the pack replaces itself about eight times in the season. With various choices for seasonal extent, velocities, and persistence, the range of possible replacements is from two to ten. It should be remembered, however, that the cycling of the pack is continuous. The number of replacements is an indication of the dynamic and thermodynamic vigor of the system.

#### SUMMARY AND CONCLUSIONS

During the winter of 1979, ice was observed to form in the northern and coastal regions of the Bering Sea, to advect south-southwesterly, and to melt along

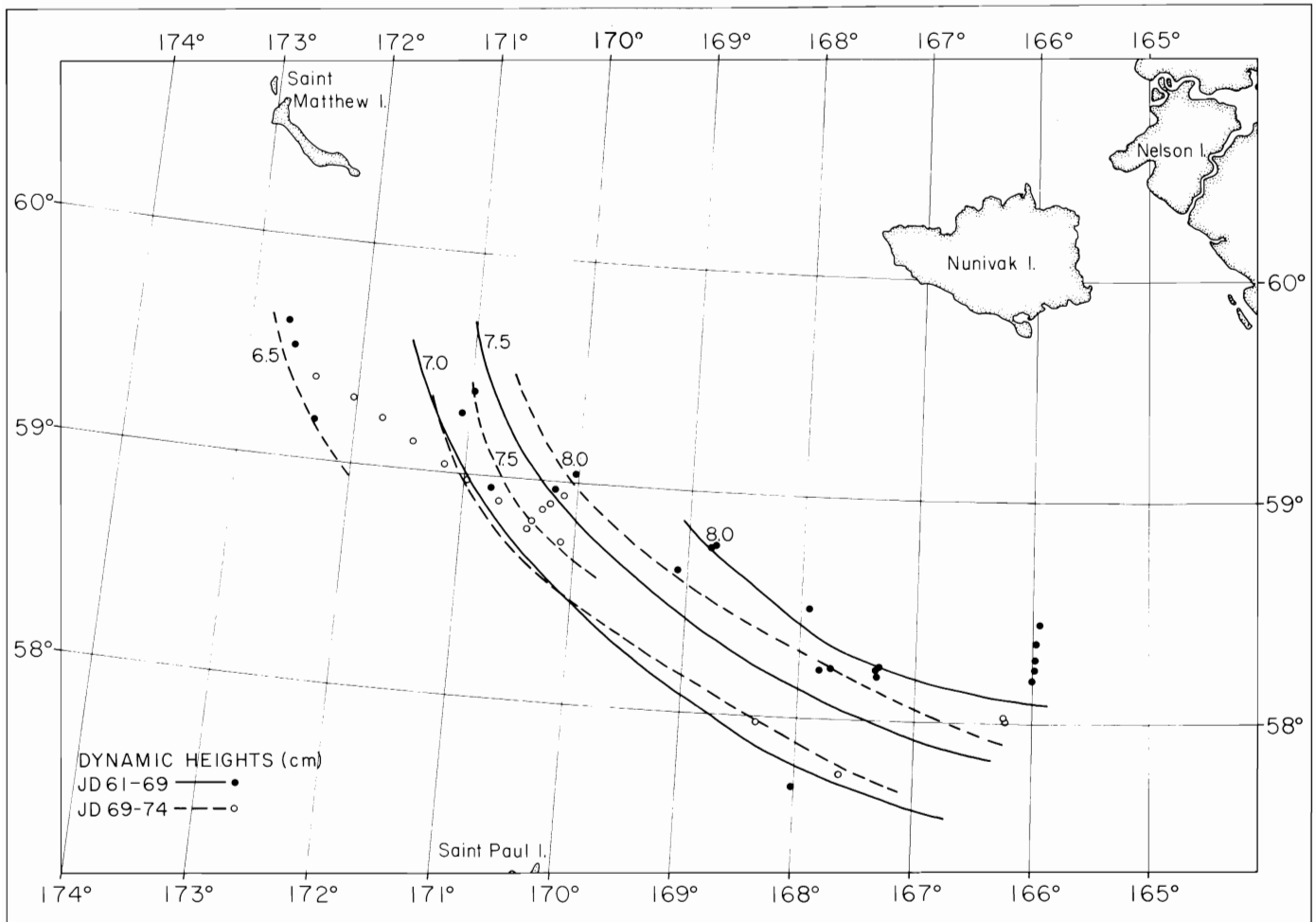


Figure 13-7. Dynamic topography between 2 March and 15 March 1979 computed from CTD stations illustrated in Fig. 13-2. Note northwesterly set of lines of constant topography. This implies a relatively weak northwesterly current.

the southern margin; ice processes over the Bering Sea shelf can thus be thought of as a conveyor belt. The interaction between the dynamic and thermodynamic processes of decay along the margin was explored for March 1979 using measurements taken from the NOAA ship *Surveyor*. This analysis and remote sensing analysis by McNutt (Chapter 10, this volume) show that the same processes were at work during 1979, an extremely light ice year, as in 1974, a medium-heavy ice year (Muench and Ahlnäs 1976). This suggests that the extent of the pack ice from one year to another is a function of both the advective scheme and thermodynamic processes.

The conveyor belt process of ice growth and decay is responsible for enhancing salt content in northern and coastal waters (ice production areas) and reducing salinity, resulting in stratified waters along the ice

margin. This process has a considerable effect on the structure of water properties of the shelf, at least during the winter season. The vigor of the advective scheme, i.e., wind blowing the ice, also affects the extent of freezing.

#### ACKNOWLEDGMENTS

This study was funded through the Marine Services Project at Pacific Marine Environmental Laboratories. The cruise time on the NOAA ship *Surveyor* was requested by the late Robert Charnell of PMEL and arranged by the OCSEAP Juneau Project Office. Dr. Seelye Martin of the Department of Oceanography at the University of Washington acted as chief scientist on the cruise. The routine oceanographic measure-

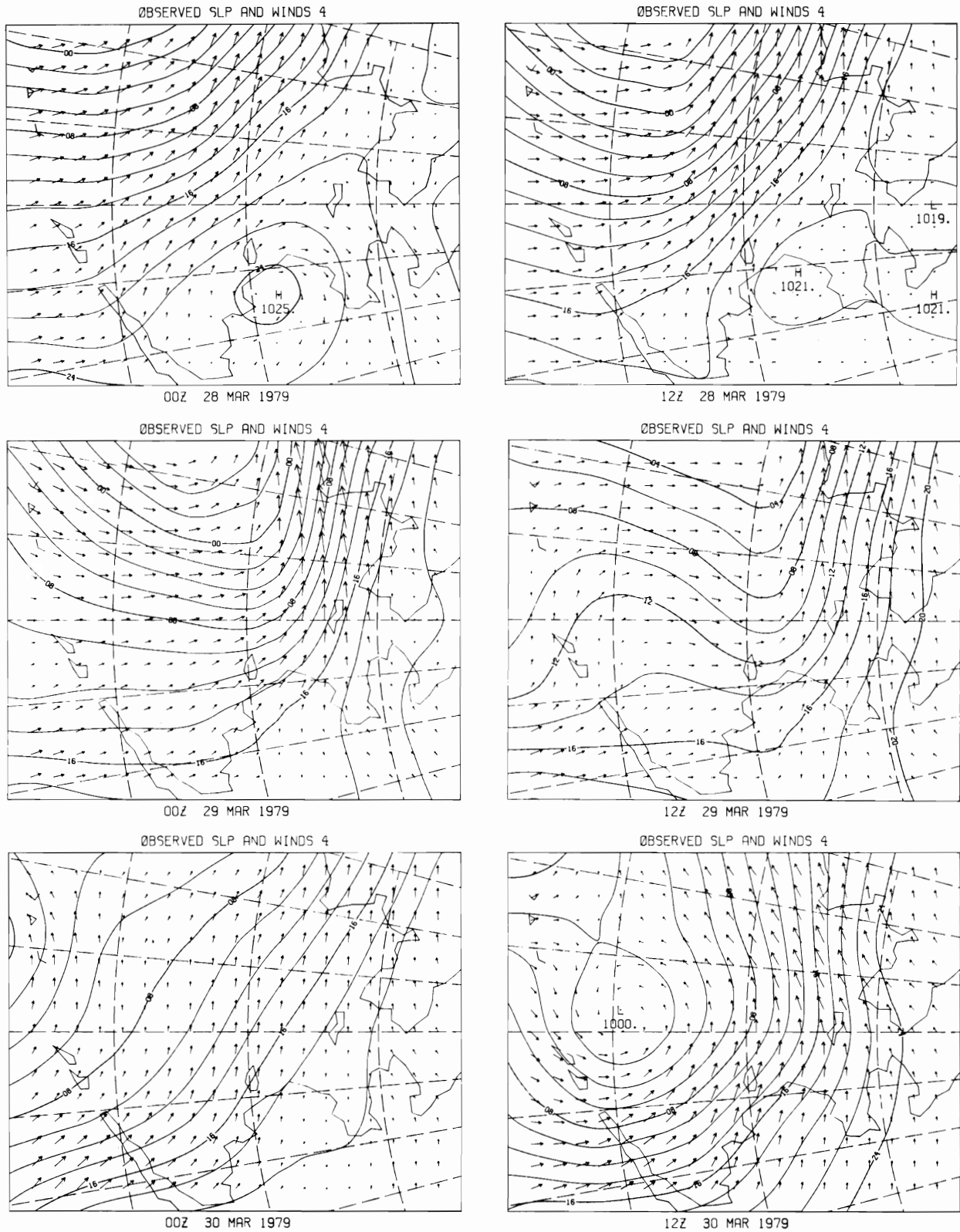


Figure 13-8. Sea-level pressure and wind fields calculated from digitized NWS-Alaska region surface analysis charts for 28, 29, and 30 March 1979. This pattern is the dominant spring condition driving the ice northerly and warming the basin. Longest vectors represent 20 m/sec winds.



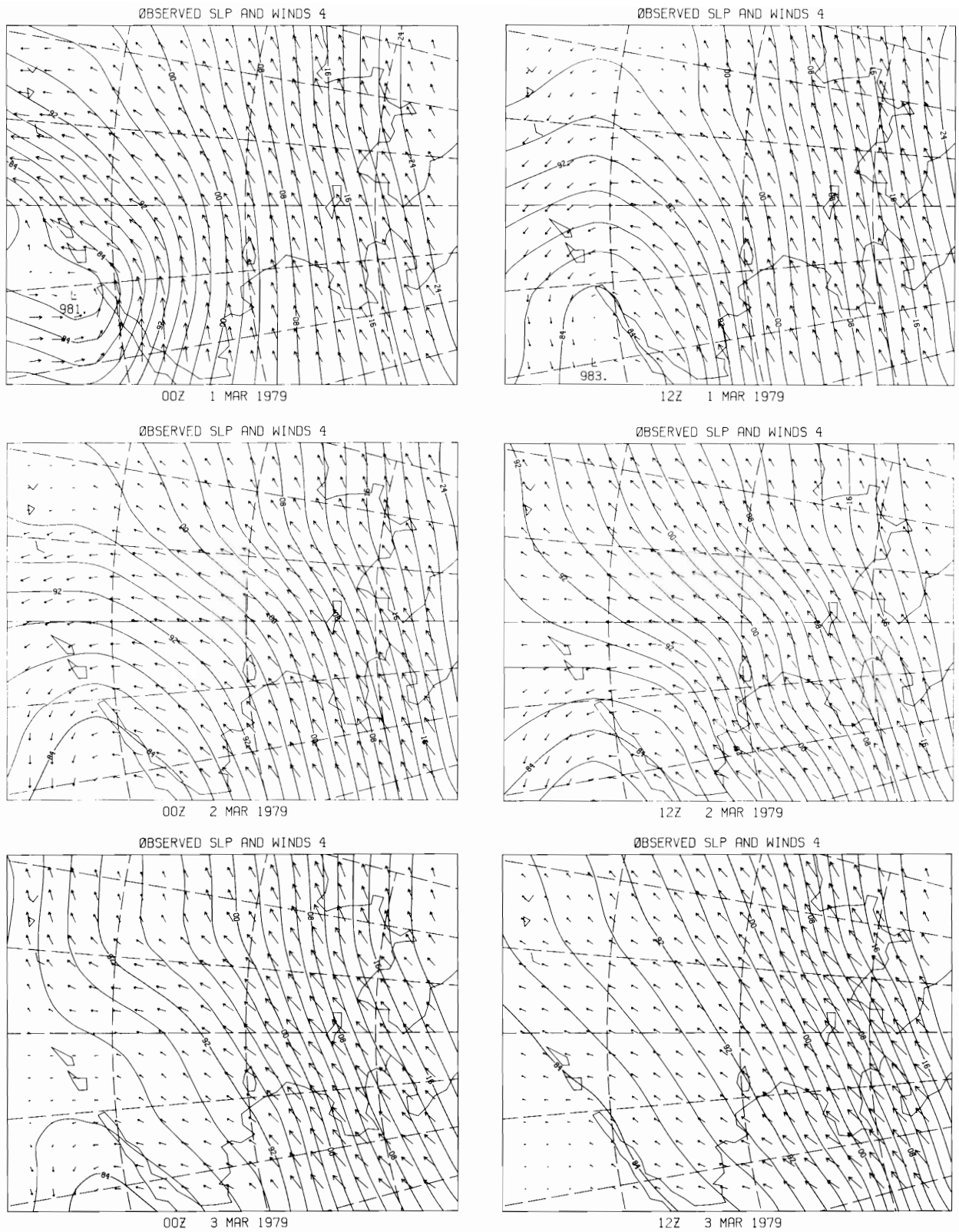


Figure 13-9. Sea-level pressure and wind fields calculated from digitized NWS-Alaska region surface analysis charts for 1, 2, and 3 March 1979. This pattern is the dominant winter condition driving the ice southwesterly and cooling the basin. Longest vectors represent 20 m/sec winds.

ments were carried out by the survey technicians on the *Surveyor*, who patiently modified their operations to meet my requirements.

Frances Parmenter of the NESS field office in Anchorage, Bruce Webster, ice forecaster for NWS Fairbanks, and Doris Brown of the NWS Anchorage office contributed materials for the field parameter analysis. Lt. (jg.) Daniel V. Munger and AGC William B. Damico flew the Navy ice reconnaissance for the

NOAA-Navy Joint Ice Center under the leadership of Comdr. James C. Langemo.

Sigrid Salo of PMEL handled much of the data analysis and prepared the figures. Joy Golly and James Anderson completed the drafting and photography. Drs. James E. Overland and James D. Schumacher discussed important aspects of the physics. Seelye Martin and Lyn McNutt were my colleagues in the experiment.



## REFERENCES

- Ahlnäs, K., and G. Wendler  
1979 Sea ice observations in the Bering, Chukchi, and Beaufort Seas. Proceedings of POAC-79, Norwegian Institute of Technology.
- Charnell, R. L., J. D. Schumacher, L. K. Coachman, and T. H. Kinder  
1979 Bristol Bay oceanographic processes. Fourth Ann. Rep. to OCSEAP, Research Units 549/141.
- Coachman, L. K., T. H. Kinder, J. D. Schumacher, and R. L. Charnell  
1978 Bristol Bay oceanographic processes. Third Ann. Rep. to OCSEAP, Research Units 141/594.
- Fleet Weather Facility  
1972-1975 Western Arctic Sea ice analysis. Capt. S. C. Balmforth, C.O. Suitland, Md.
- 1976 Eastern-western Arctic Sea ice analysis. Comdr. V. W. Roper, C.O., Suitland, Md.
- 1977 Eastern-western Arctic Sea ice analysis. Capt. J. A. Jepson, C.O. Suitland, Md.
- 1978 Eastern-western Arctic Sea ice analysis. Comdr. J. D. Langemo, C.O., Suitland, Md.
- Martin, S., and P. Kauffman  
1979 Data report on the ice cores taken during the March 1979 Bering Sea ice edge field cruise on the NOAA ship *Surveyor* (Sept. 14, 1979). Univ. of Washington, Dep. of Oceanogr. Spec. Rep. 89.
- Muench, R. D., and K. Ahlnäs  
1976 Ice movement and distribution in the Bering Sea from March to June 1974. *J. Geophys. Res.* 81 (24): 4467-76.
- Parmenter, P. R., and M. D. Coon  
1973 Mechanical models of ridging in the Arctic sea ice cover, *AIDJEX Bull.* 19: 59-112.

